2024 Tenth Indian Control Conference (ICC)
9 - 11 December, 2024
IISER Bhopal, India

Minimum Operator Based Discrete-Time Nonlinear Observer Design for the State of Charge Estimation of Li-ion Battery

Shilpi Shiwangi[1] , Sunidhi Pandey[1], Sandip Ghosh[1], Shyam Kamal[1], J C Pandey[1], and Eram Taslima[1]

***Abstract*— This paper introduces a novel minimum operator-based discrete-time nonlinear observer for estimating the online state of charge (SoC) of Li-ion batteries. This observer ensures finite-time estimation error convergence. The battery's model employs a second-order resistor-capacitor (2-RC) equivalent circuit, where the parameters are determined via a least-squares fitting method and treated as nonlinear functions. The Lyapunov direct method is used to demonstrate the finite-time convergence of the estimation error in discrete time. The proposed method's performance is validated under hybrid pulse power characterization (HPPC) and urban dynamometer driving schedule (UDDS) conditions. Simulation and experimental results show that it provides better estimation accuracy and tracking capability than existing discrete-time nonlinear observers.**

I. Introduction

Lithium-ion batteries (LIBs) are increasingly favored for their high energy density, extended durability, and eco-friendly attributes, making them highly sought-after in both energy storage solutions and electric mobility applications. [1]. Effective management of LIBs requires a Battery Management System (BMS) to continuously monitor internal conditions, ensuring operational safety. The SOC indicates the remaining useful charge of the battery and the determination of SoC is the main task of BMS [2].

Accurately estimating the SoC of the battery, required precise modelling of the battery. The modeling of LIBs entails creating mathematical representations that capture the electrochemical dynamics of the battery throughout its charge and discharge cycles. In the current scenario, the most common modelling of batteries are the electrochemical model (EM) [3], neural network model [4], and equivalent circuit model (ECM) [5]–[8]. The electrochemical modelling captures all phenomena such as diffusion, migration, and electrochemical reactions so, it is an accurate representation of the model however the model is complex and time-consuming therefore it can't integrate with BMS. The neural network model, while uncomplicated and user-friendly, was built upon a significant dataset gathered from extensive experimentation. The equivalent circuit model (ECM) of the battery is solely based on its steady-state and transient behaviors, determined through a series of tests conducted under different loading conditions. This model considers the battery's characteristics as equivalent, making analysis straightforward and computationally efficient. Owing to its simplicity and excellent computational efficiency, the ECM model is the most appropriate for estimating the SoC of LIBs compared to other models.

Various techniques have been proposed to estimate the SoC of LIBs, including the ampere-hour (Ah) counting method, Kalman filter (KF), machine learning-based technique, support vector machine (SVM), Lyapunov-based method, discrete-time sliding mode observer (DSMO) and discrete-time nonlinear observer (DNLO) method. The ampere-hour (Ah) counting method is a widely used and simple technique to implement, but it depends on an accurate initial SoC and precise current measurement sensors [9]. The KF and its variations are commonly employed in research studies to manage the substantial non-linearity of battery models. However, these techniques demand substantial computational time and some information about system noise [10], [11]. Machine learning techniques [12], including SVM [13], yield promising results with high accuracy. However, they demand superior, diverse, and abundant training data, making them challenging to implement in real-time applications. In [14], a straightforward battery model was employed to develop a Lyapunov-based method for estimating SoC. The primary limitation of this method is that it can only guarantee asymptotic estimation of the states. A DSMO [15] was developed for SoC estimation in discrete-time battery systems but, like conventional SMOs, it necessitates linearizing the nonlinear OCV-SoC system, causing substantial model errors. A DNLO from [16] was used for SoC estimation in batteries. A key feature is that its gain matrix is a function of SoC, providing strong resilience to external disturbances and parameters. However, it estimates states asymptotically, leading to higher estimation errors.

All the techniques discussed in the above paragraph show asymptotic convergence of estimation error. Recently non-asymptotic convergence of trajectories is an ongoing field of research among control theorists. Finite/fixed-time convergence of trajectories of discrete time dynamical systems is a less explored area compared to continuous time systems. Recently some authors [17]–[21] discussed thoroughly the finite-time convergence of discrete-time autonomous systems using a minimum operator.

Motivated by this, we propose a minimum operator-based finite-time convergent discrete-time nonlinear observer. To the best of the author's knowledge, this paper is the first to investigate the finite-time convergence (FTC) of estimation

This work was supported by the project titled "Center for Development of Drone Related Technologies (CDRT)", IIT (BHU) Varanasi, India under grant (No. R & $D/SA/I-DAPTIIT(BHU)/EE/22-23/08/448$).

[1]Shilpi Shiwangi, Sunidhi Pandey, Sandip Ghosh, Shyam Kamal, J C Pandey, and Eram Taslima are with the Department of Electrical Engineering, IIT(BHU) Varanasi, India, shilpishiwangi.rs.eee21@iitbhu.ac.in, sunidhipandey.rs.eee20@iitbhu.ac.in, sghosh.eee@iitbhu.ac.in, shyamkamal.eee@iitbhu.ac.in, jcpandey.eee@iitbhu.ac.in, eramtaslima.rs.eee21@itbhu.ac.in

error using a DNLO. A proof derived from Lyapunov's direct method is presented to demonstrate the FTC characteristic of the proposed observer. Finally, the simulation outcomes illustrate the effectiveness of the minimum operator-based designed observer, showcasing improved estimation accuracy and a more rapid convergence rate.

The subsequent sections of the paper are arranged as follows: Section II describes the notation and preliminaries. Section III introduced the modelling of Lithium-ion battery and their parameter identification method. Section IV presents the design of a minimum operator-based discrete-time nonlinear observer for SOC estimation and demonstrates its stability and convergence. Section V discusses the experimental and simulation results. Finally, Section VI provides the conclusions.

II. Notations and Preliminaries

A. Notation

$\mathbb{R}, \mathbb{R}_{>0}$ and $\mathbb{R}^m$ be the fields of real numbers, positive real numbers, and m dimensional Euclidean space over the field $\mathbb{R}$ respectively. $\mathbb{Z}$ denotes the set of nonnegative integers. $\|\cdot\|$ denote Euclidean norm. max and min denote the greatest element and smallest of the set respectively. $(\cdot)^\top$ refers to the transpose. We write $\Delta V(x)$ for the difference operator of $V : \mathbb{R}^n \to \mathbb{R}$ at x, $\lceil b \rceil$ for ceiling function which denotes the smallest integer greater than or equal to b, $\lfloor b \rfloor$ for floor function which denotes the greatest integer lesser than or equal to b.

B. Preliminaries

Consider the following dynamics

$$x(k+1) = g(x(k)), \quad x(0) = x_0, \quad k \in \mathbb{Z}, \tag{1}$$

where, $k \in \mathbb{Z},\ x(k) \subset \mathcal{D} \in \mathbb{R}^n, 0 \in \mathcal{D}, g : \mathcal{D} \to \mathcal{D}, g(0) = 0$

Definition 1: Consider the dynamics (1), and let the solution sequence be defined as $x(k) = l(k, x_0)$. The zero solution $x(k) \equiv 0$ of (1) is finite/fixed-time stable if there exists an open neighborhood of origin ($\mathcal{N} \subset \mathcal{D}$) and a settling-time function ($\mathcal{K} : \mathcal{N} \to \mathbb{Z}$) s.t.:

(a) **Lyapunov stability:** $\forall\ \epsilon > 0, \exists\ \delta > 0$ s.t. $\forall\ x \in \mathcal{B}_\delta(0)\backslash\{0\}$, where, $\mathcal{B}_\delta(0) \in \mathcal{N}, \exists\, l(k, x_0) \in \mathcal{B}_\epsilon(0)\ \forall k \in \{0, ..., \mathcal{K} - 1\}$.

(b) **Finite-time convergence (FTC):** $\forall\ x \in \mathcal{N}\backslash\{0\}$ and $k > \mathcal{K},\ l(k, x_0)$ is in $\mathcal{N} \cap \{0\}$.

Lemma 1: [17] Consider the dynamics (1). Let $\exists$ a continuous function $\mathcal{V} : \mathcal{D} \to \mathbb{R}$, $m \in \mathbb{R}_{>0}, \alpha \in (0, 1)$ and a neighbourhood of the origin ($\mathcal{N} \subseteq \mathcal{D}$) s.t.: (a) $\mathcal{V}(0) = 0$, (b) $\mathcal{V}(x) > 0,\ x \in \mathcal{N}\backslash\{0\}$, (c) $\Delta\mathcal{V}(x) \leq -\min\{\mathcal{V}, \mathcal{V}^\alpha\},\ \ x \in \mathcal{N}\backslash\{0\}$. Then the zero solution is FTS. Moreover, if $\mathcal{N} = \mathcal{D} = \mathbb{R}^n$ and $\mathcal{V}$ is radially unbounded then zero solution is globally FTS.

III. Modeling of Lithium-ion Battery

A. Equivalent Circuit Model (ECM) of Battery

Based on the steady-state and transient behavior of the battery, the ECM is designed by using resistors, capacitors, and voltage sources such as the Rint model (n=0) [5], the first order (1-RC) model (n=1) [8], the second order (2-RC) model (n=2) [6] and many more parallel RC- branch can be connected to develop the n-RC model. The precision of the model improves as the number of RC branches in the ECM rises, but more complex models are produced. In this paper, the 2- RC model is taken into consideration for accuracy and complexity reasons which is shown in Fig1. The 2- RC model incorporates an open-circuit voltage source (V_{oc}), represents the thermodynamic equilibrium potential, a resistance (R_0) accounting for internal voltage drop and 2-RC parallel branch (R_1, C_1 and R_2, C_2) describe the transient characteristic of battery[8]. The measurable quantities are the input current I_L and terminal voltage V_t.

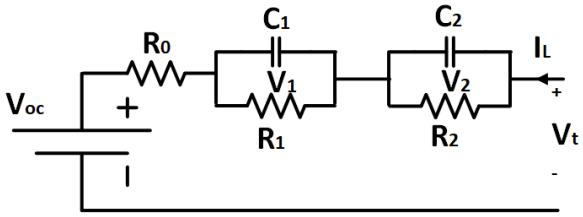


Fig. 1: 2- RC model

Apply the KCL and KVL in the second order ECM as shown in Fig1 and get the following expression written as below:

$$\begin{cases} \dot{V_1} = -\frac{1}{R_1 C_1} + \frac{1}{C_1} \\ \dot{V_2} = -\frac{1}{R_2 C_2} + \frac{1}{C_2} \end{cases} \tag{2}$$

$$V_t = V_{oc}(SoC) - V_1 - V_2 - R_0 I_L \tag{3}$$

Where V_1 and V_2 are the voltage across the parallel branches (R_1, C_1) and (R_2, C_2) respectively; and V_{oc} is a monotonic function of SoC. According to Coulomb counting SoC is defined as below:

$$SoC(t) = SoC(t_0) - \frac{1}{C_b} \int_{t_0}^{t} I_L(\tau)\, d\tau \tag{4}$$

Where $SoC(t_0)$ is the initial SoC and C_b is the battery's rated capacity

B. Parameter Identification of Battery Model

Accurate identification of the parameters of the model plays a critical role in the estimation of SoC. The least-square fitting approach is used to estimate the parameter of the 2-RC model of LIB. To apply the least square estimation (LSE) on the ECM model, an autoregressive exogenous (ARX) model is required [22]. Thus apply the Laplace transform on equation (2) and obtain the frequency domain transfer function as follows:

$$\frac{V_{OC}(s) - V_t(s)}{I_L(s)} = R_0 + \frac{R_1}{1 + R_1 C_1 s} + \frac{R_2}{1 + R_2 C_2 s} \tag{5}$$

Time constant are $\tau_1 = R_1 C_1,\ \ \tau_2 = R_2 C_2$ and assume that $V(s) = V_{OC}(s) - V_t(s),\ \ a_1 = \tau_1 \tau_2,\ \ b_1 = \tau_1 + \tau_2,\ \ c_1 =$

TABLE I: Estimated parameters of 2-RC model

SoC	$R_0(m\Omega)$	$R_1(m\Omega)$	$C_1(kF)$	$R_1(m\Omega)$	$C_2(kF)$
0	3.26	8.87	0.49	2.25	10.23
.1	4.42	1.78	1.04	1.07	22.15
.2	4.10	1.06	1.79	1.04	24.55
.3	3.89	0.78	2.50	0.89	30.10
.4	4.02	0.63	3.82	0.81	36.25
.5	4.27	0.65	2.88	0.79	34.80
.6	3.94	0.65	3.72	0.74	39.75
.7	3.90	0.71	3.29	0.94	34.80
.8	3.92	0.79	2.97	0.97	31.00
.9	4.34	0.77	2.40	0.85	30.85
1	4.17	0.94	2.51	0.81	35.75

$R_0 + R_1 + R_2, \quad d_1 = (R_0 + R_1)\tau_2 + (R_0 + R_2)\tau_2$. Then (5) is rewritten as below:

$$\frac{V(s)}{I_L(s)} = -\frac{a_1 R_0 s^2 + d_1 s + c_1}{a_1 s^2 + b_1 s + 1} \tag{6}$$

Apply the bi-linear transform $s = \frac{2(1-z^{-1})}{T(1+z^{-1})}$ to transform the frequency domain transfer function (6) to discrete time transfer function as follows:

$$\frac{V(z^{-}1)}{I_L(z^{-}1)} = -\frac{k_3 + k_4 z^{-}1 + k_5 z^{-}2}{1 - k_1 z^{-}1 - k_2 z^{-}2} \tag{7}$$

Difference equation of terminal voltage $V_t(k)$ can obtain from (7) as below:

$$\begin{aligned} V_t(k) = k_1 V_t(k-1) + k_2 V_t(k-2) + k_3 I_L(k) \\ + k_4 I_L(k-1) + k_5 I_L(k-2) \end{aligned} \tag{8}$$

Equation (8) can also be written in vector form as below:

$$V_t(k) = A(k)^T K(k) \tag{9}$$

Where $A(k) = [V_t(k-1),\ V_t(k-2),\ I_L(k),\ I_L(k-1),\ I_L(k-2)]$ and $K(k) = [k_1,\ k_2,\ k_3,\ k_4,\ k_5]$.
Now apply the LSE to the equation (9) and obtain the parameter vector $K(k)$ of model as below:

$$K(k) = [A(k)^T A(k)]^{-1} A(k)^T V_t(k) \tag{10}$$

As a result, the model's estimated parameters are acquired as shown in table I. Each parameter is obtained for each cycle of the HPPC test, each cycle uses 10% of SoC and details of the HPPC test will be explained in section IV. The values of parameters R_0, R_1, C_1, R_2 and C_2 of the model are obtained by using the LSE whereas V_{oc} and SoC relationship is as presented in [16].

$$\begin{aligned} V_{oc}(SoC) = -327.932SoC^9 + 1248.695SoC^8 \\ -1826.955SoC^7 + 1213.788SoC^6 - 255.813SoC^5 \\ -112.496SoC^4 + 76.748SoC^3 - 17.736SoC^2 \\ +2.523SoC^1 + 3.358 \end{aligned} \tag{11}$$

A ninth-order polynomial, equation (11) characterizes the highly nonlinear correlation between OCV and SoC.

IV. Minimum operator-based discrete-time nonlinear observer for SoC estimation

A. Minimum Operator-based Discrete-time Nonlinear Observer

Based on (2) and (5) of the model, the discrete-time formulation of the state space model for estimating SoC is derived as follows:

$$\begin{aligned} x(k+1) &= \begin{bmatrix} e^{-\frac{T}{R_1 C_1}} & 0 & 0 \\ 0 & e^{-\frac{T}{R_2 C_2}} & 0 \\ 0 & 0 & 1 \end{bmatrix} x(k) \\ &+ \begin{bmatrix} (1 - e^{-\frac{T}{R_1 C_1}}) R_1 \\ (1 - e^{-\frac{T}{R_2 C_2}}) R_2 \\ -\frac{T}{C_b} \end{bmatrix} I_L(k) \\ y(k+1) &= \begin{bmatrix} -1 & 0 \end{bmatrix} x(k+1) \\ &+ V_{oc}(k+1) - R_0 I_L(k+1) \end{aligned} \tag{12}$$

Where $x(k+1) = [V_1(k+1),\ V_2(k+1),\ SoC(k+1)]$ and $x(k) = [V_1(k),\ V_2(k),\ SoC(k)]$ are state variables at time step $k+1$ and k, respectively; $y(k+1) = [V_t(k+1)]$ is output variable at time step $k+1$; T is sampling time, and $T = 1$second is taken in this paper. The model parameters fluctuate with changes in the battery's SoC, therefore the standard form of state space representation:

$$x(k+1) = F(k)x(k) + G(k)I_L(k) \tag{13}$$

Where $F(k) = \begin{bmatrix} L_1(k) & 0 & 0 \\ 0 & L_2(k) & 0 \\ 0 & 0 & 1 \end{bmatrix}$; $L_1(k) = e^{-\frac{T}{R_1 C_1}}$;

$L_2(k) = e^{-\frac{T}{R_2 C_2}}$; $\quad G(k) = \begin{bmatrix} (1 - e^{-\frac{T}{R_1 C_1}}) R_1 \\ (1 - e^{-\frac{T}{R_2 C_2}}) R_2 \\ -\frac{T}{C_b} \end{bmatrix}$

Based on terminal voltage equation (3), output expression can be formulated as:

$$V_t = Q(x) + I_L R_0 \tag{14}$$

Where $Q(x) = V_{oc} + V_1 + V_2$.
The derivative of $Q(x)$ can be written as below:

$$\dot{Q(x)} = \begin{bmatrix} \frac{\partial Q(x)}{\partial V_1} & \frac{\partial Q(x)}{\partial V_2} & \frac{\partial Q(x)}{\partial SoC} \end{bmatrix} = [1 \quad 1 \quad Q_3] \tag{15}$$

In the output equation (5), V_{oc} is a nonlinear function of SoC therefore minimum operator-based discrete-time nonlinear observer for state equation (13) is design as below:

$$\begin{aligned} \hat{x}(k+1) = F(k)\hat{x}(k) + G(k)I_L(k) - M\text{Sign}(\tilde{V_t}) \\ min((M\dot{Q}(\hat{x}(k))^{-1}|\tilde{V_t}|, |\tilde{V_t}|^{\alpha}) \end{aligned} \tag{16}$$

where the gain matrix $M = \begin{bmatrix} m_1 L_1(k) & 0 & 0 \\ 0 & m_2 L_2(k) & 0 \\ 0 & 0 & m_3 \end{bmatrix} \in \mathbb{R}^{n \times n}$ is a positive definite matix; m_1, m_2, and m_3 are all undetermined positive constants; and $\hat{x}$ is estimated states. $\tilde{V_t} = V_t - \hat{V_t},\ x \in \mathbb{R}^n, I_L \in \mathbb{R}^m, |\tilde{V_t}| = [|\tilde{V_t}|, \ldots, |\tilde{V_t}|]^T \in \mathbb{R}^{n \times 1}, |\tilde{V_t}|^{\alpha} = [|\tilde{V_t}|^{\alpha}, \ldots, |\tilde{V_t}|^{\alpha}] \in \mathbb{R}^{n \times 1}, F \in \mathbb{R}^{n \times n}, B \in \mathbb{R}^{n \times m}$, $\text{Sign}\left(\tilde{V_t}\right) = diag\left(\text{sign}(\tilde{V_t}), \ldots, \text{sign}(\tilde{V_t})\right) \in \mathbb{R}^{n \times n}$

and $0 < \alpha < 1$.
In the feedback, the factor $M\dot{Q}(X(k))$ is a function of states that prevents the disturbance from affecting the estimation state of the system.

B. Stability Analisis

The dynamic of the state estimation error can be obtained by subtracting the equation (16) and (13) as follows:

$$\begin{aligned} e(k+1) =& \hat{x}(k+1) - x(k+1) \\ =& F(k)e(k) - M\dot{Q}(x(k))\text{Sign}(\tilde{V}_t) \\ & min((M\dot{Q}(x(k)))^{-1}|\tilde{V}_t|, |\tilde{V}_t|^{\alpha}) \end{aligned} \tag{17}$$

Theorem 1: Consider the dynamics of estimation error (17). Let there exist a continuous function $V : \mathbb{R}^n \to \mathbb{R}_{>0}$ which satisfies (a) $V(e) > 0$, (b) $V(e = 0) = 0$, and (c) $\Delta V \leq -min(V(e(k), \Lambda_{min}(M^T M)V^{\alpha}(e(k))),\ \forall e \in \mathcal{N}\backslash\{0\}$, where $\Lambda_{min}(M^T M)$ denotes minimum eigen-value of the matrix $M^T M$. Then, $e(k) \equiv 0$ is finite-time stable.

Proof: We show the finite-time convergence of the error dynamics (17) by considering a Lyapunov function candidate as $V(e(k)) = e^T(k)e(k)$. To carry out the analysis using Lyapunov's direct method, we take an increment of V(e(k)) as:

$$\begin{aligned} \Delta V(e(k)) =& V(e(k+1)) - V(e(k)) \\ =& e^T(k+1)e(k+1) - e^T(k)e(k) \\ =& e^T(k)F^T(k)F(k)e(k) - 2e^T(k)F(k) \\ & M\text{Sign}(e(k))min(M^{-1}|e(k)|, |e(k)|^{\alpha}) \\ & + min(M^{-1}|e(k)|, |e(k)|^{\alpha})M^2 \\ & min(M^{-1}|e(k)|, |e(k)|^{\alpha}) - e^T(k)e(k) \\ =& e^T(k)(F^T(k)F(k) - I)e(k) - 2e^T(k) \\ & (-F^T(k) + I)\text{Sign}(e(k))min(M^{-1}|e(k)|, |e(k)|^{\alpha}) \\ & - 2e^T(k)M\text{Sign}(e(k))min(M^{-1}|e(k)|, |e(k)|^{\alpha}) \\ & + min(M^{-1}|e(k)|, |e(k)|^{\alpha})M^2 \\ & min(M^{-1}|e(k)|, |e(k)|^{\alpha}) \end{aligned} \tag{18}$$

Where $|e(k)| = (|e_1(k)|, \ldots, |e_n(k)|)$ and $|e(k)|^{\alpha} = (|e_1(k)|^{\alpha}, \ldots, |e_n(k)|^{\alpha})^T$.
As $(F^T(k)F(k) - I) < 2(-F^T(k) + I)$. Let, $|e(k)|^{\alpha-1} \leq \kappa$ (It means that each element of $|e(k)|^{\alpha-1} = (|e_1(k)|^{\alpha-1}, \ldots, |e_n(k)|^{\alpha-1})$ is less than some constant value κ) and assume that $(F^T(k)F(k) - I) < 2\kappa(-F^T(k) + I)M$ then equation (18) can be written as:

$$\begin{aligned} \Delta V(e(k)) \leq & -2|e|^T M min(M^{-1}|e(k)|, |e(k)|^{\alpha}) + \\ & min(M^{-1}|e(k)|, |e(k)|^{\alpha})M^2 \\ & min(M^{-1}|e(k)|, |e(k)|^{\alpha}) \\ =& -(2|e|^T M - min(M^{-1}|e(k)|, |e(k)|^{\alpha})^T M^2) \\ & min(M^{-1}|e(k)|, |e(k)|^{\alpha}) \\ \leq & -min(M^{-1}|e(k)|, |e(k)|^{\alpha})^T M^T M \\ & min(M^{-1}|e(k)|, |e(k)|^{\alpha}) \\ =& -min(|e(k)|^T|e(k)|, |e(k)|^{\alpha}|M^T M e(k)|^{\alpha}) \\ \leq & -min(V(e(k), \Lambda_{min}(M^T M)V^{\alpha}(e(k))) \end{aligned} \tag{19}$$

Therefore, considering Lemma 1 and (19), we can conclude that error dynamics (17) is FTC or $\lim_{k \to T_0} e(k) = 0$ where T_0 is the settling time which means that error system is stabilized in finite time and estimated state will converge to the true state. ■

V. EXPERIMENTAL RESULTS AND COMPARISON

A. Experimental Setup

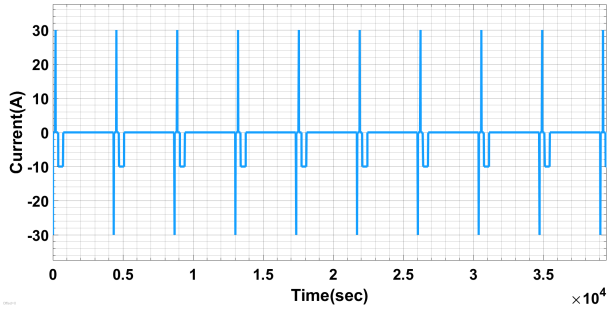
In this section, the HPPC test and UDDS test conditions are selected to perform the test on a LIB at room temperature (24 degrees Celsius), and the basic specification of LIB is also shown in table II. In the case of the HPPC test as shown in Fig (2) each cycle follows steps: (1) Discharge by $3C_b$ rate for 10second; (2) Rest for 180second; (3) Charge by $3C_b$ rate for 10second; (4) Rest for 180 seconds; and (5) Discharge by $1C_b$ for 360 seconds, Subsequently, there is a 3600 seconds intermission to allow the battery to return to equilibrium before commencing the next cycle, with each cycle decreasing the SoC of the battery by 10%. The load current and terminal voltage are also shown in Fig (6) under the condition of the UDDS test.

TABLE II: Descriptions of Li-ion battery (LIB)

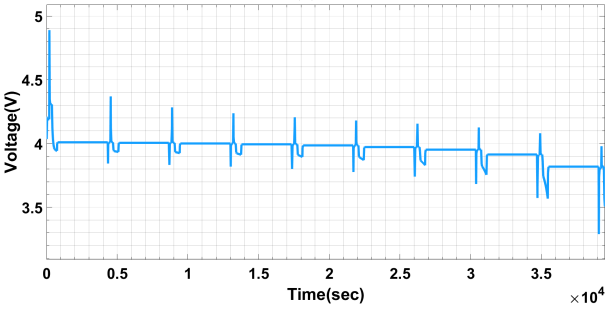
Cell	Li-ion battery.
Rated capacity(C_b)	10Ah
Nominal Voltage (V)	3.7V
Discharge cut-off voltage	2.7V
Initial SOC	100%

B. Comparison of SoC under Different Test Conditions

To verify the performance of the proposed observer, compared with the well-established DNLO method [16]. Based on the current profile, the reference value of the battery's SoC is obtained using the ampere-hour integration method. Under the HPPC test condition, the estimated SoC results of the proposed observer and DNLO are shown in Fig (4(a)), and their estimated errors are also shown in Fig (4(b)). The UDDS cycle profile is also utilized to verify the proposed SoC estimation method and DNLO method. Fig (5) shows the comparison of the estimated SoC and estimated SoC error by the proposed method and DNLO method under the UDDS test condition. In all test conditions, comparison results show

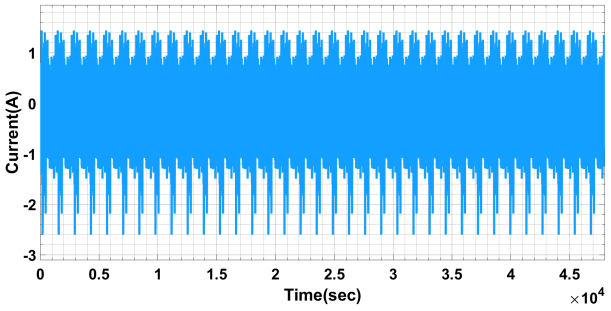


(a)

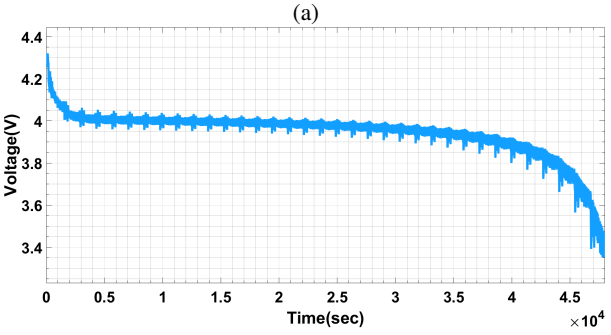


(b)

Fig. 2: Under HPPC condition:(a) input current; (b) voltage

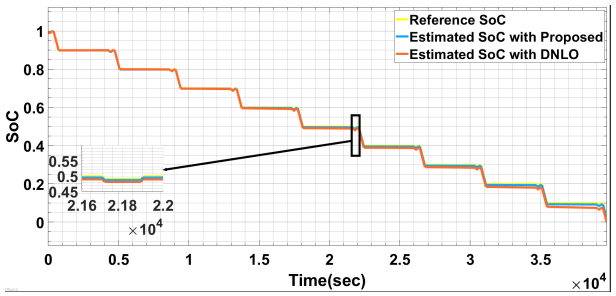


(a)

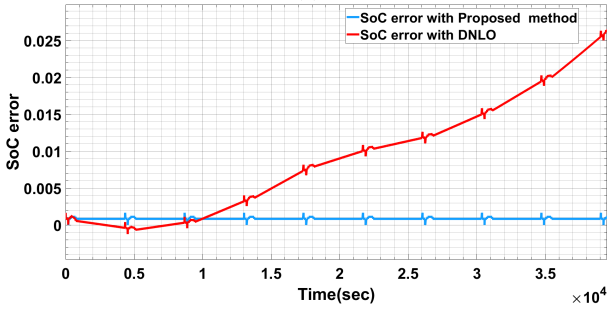


(b)

Fig. 3: Under UDDS condition:(a) input current; (b) voltage



(a)



(b)

Fig. 4: Under HPPC condition:(a) estimated SoC; (b) SoC error

that the proposed method tracks the reference SoC more quickly and accurately as compared to the DNLO method. Further more thoroughly investigating the accuracy of methods, considered the mathematical statistical results of an estimated error are represented in Table III which consists of maximum error, Mean Absolute Error (MAE), and Root Mean Square Error (RMSE). From Table III, the maximum SoC error for the proposed method is 33.33% and 61% less than the NDLO method under the test condition of HPPC and UDDS respectively. This illustrates that the proposed method attains greater estimation accuracy compared to the NDLO method.

VI. Conclusion

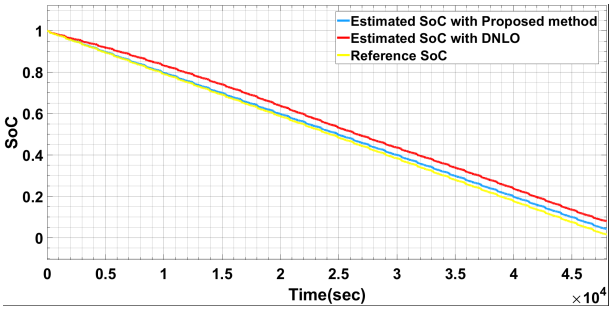
A minimum operator-based discrete-time nonlinear observer design method has been presented in this paper for estimating the SoC of LIB. A 2- RC model was used to model the battery and the model's parameter was estimated by LSE. The Lyapunov direct method has been involved in establishing the proof of convergence and stability of the proposed method. The performance of a proposed method has been verified under two test conditions i.e. HPPC and UDDS. In both test conditions, the results demonstrate that the proposed method effectively tracks and achieves accurate estimation as compared to the DNLO method.

References

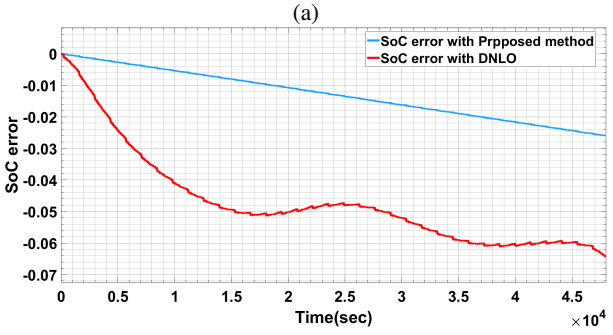
[1] H. Rahimi-Eichi, U. Ojha, F. Baronti, and M.-Y. Chow, "Battery management system: An overview of its application in the smart grid and electric vehicles," *IEEE industrial electronics magazine*, vol. 7, no. 2, pp. 4–16, 2013.

TABLE III: SoC estimation error results

Condition	Method of SoC estimation	Maximum Error(V)	MAE(V)	RMSE(V)
HPPC	SoC estimated with proposed method	2.1×10^{-3}	8.564×10^{-4}	8.62×10^{-4}
	DNLO	3×10^{-2}	9.1×10^{-3}	1.1866×10^{-2}
UDDS	SoC estimated with proposed method	2.5×10^{-2}	1.3×10^{-2}	1.5×10^{-2}
	DNLO	6.4×10^{-2}	4.71×10^{-2}	4.94×10^{-2}



(a)



(b)

Fig. 5: Under UDDS condition:(a) estimated SoC; (b) SoC error

[2] L. Lu, X. Han, J. Li, J. Hua, and M. Ouyang, "A review on the key issues for lithium-ion battery management in electric vehicles," *Journal of power sources*, vol. 226, pp. 272–288, 2013.

[3] T. Wang, K.-J. Tseng, S. Yin, and X. Hu, "Development of a one-dimensional thermal-electrochemical model of lithium ion battery," in *IECON 2013-39th Annual Conference of the IEEE Industrial Electronics Society*. IEEE, 2013, pp. 6709–6714.

[4] C. Zhang, Z. Yang, and K. Li, "Modeling of electric vehicle batteries using rbf neural networks," in *2014 International Conference on Computing, Management and Telecommunications (ComManTel)*. IEEE, 2014, pp. 116–121.

[5] W. He, N. Williard, C. Chen, and M. Pecht, "State of charge estimation for electric vehicle batteries using unscented kalman filtering," *Microelectronics Reliability*, vol. 53, no. 6, pp. 840–847, 2013.

[6] H. He, R. Xiong, X. Zhang, F. Sun, and J. Fan, "State-of-charge estimation of the lithium-ion battery using an adaptive extended kalman filter based on an improved thevenin model," *IEEE Transactions on vehicular technology*, vol. 60, no. 4, pp. 1461–1469, 2011.

[7] J. Lee, O. Nam, and B. Cho, "Li-ion battery soc estimation method based on the reduced order extended kalman filtering," *Journal of power sources*, vol. 174, no. 1, pp. 9–15, 2007.

[8] X. Hu, S. Li, and H. Peng, "A comparative study of equivalent circuit models for li-ion batteries," *Journal of Power Sources*, vol. 198, pp. 359–367, 2012.

[9] K. S. Ng, C.-S. Moo, Y.-P. Chen, and Y.-C. Hsieh, "Enhanced coulomb counting method for estimating state-of-charge and state-of-health of lithium-ion batteries," *Applied energy*, vol. 86, no. 9, pp. 1506–1511, 2009.

[10] H.-T. Lin, T.-J. Liang, and S.-M. Chen, "Estimation of battery state of health using probabilistic neural network," *IEEE transactions on industrial informatics*, vol. 9, no. 2, pp. 679–685, 2012.

[11] M. Charkhgard and M. Farrokhi, "State-of-charge estimation for lithium-ion batteries using neural networks and ekf," *IEEE transactions on industrial electronics*, vol. 57, no. 12, pp. 4178–4187, 2010.

[12] W. Shen, C. Chan, E. Lo, and K. Chau, "A new battery available capacity indicator for electric vehicles using neural network," *Energy Conversion and Management*, vol. 43, no. 6, pp. 817–826, 2002.

[13] J. C. A. Anton, P. J. G. Nieto, C. B. Viejo, and J. A. V. Vilán, "Support vector machines used to estimate the battery state of charge," *IEEE Transactions on power electronics*, vol. 28, no. 12, pp. 5919–5926, 2013.

[14] H. Chaoui, N. Golbon, I. Hmouz, R. Souissi, and S. Tahar, "Lyapunov-based adaptive state of charge and state of health estimation for lithium-ion batteries," *IEEE Transactions on Industrial Electronics*, vol. 62, no. 3, pp. 1610–1618, 2014.

[15] M.-W. Thein, "A discrete time variable structure observer for uncertain systems with measurement noise," in *Proceedings of the 41st IEEE Conference on Decision and Control, 2002.*, vol. 3. IEEE, 2002, pp. 2582–2587.

[16] W. Li, L. Liang, W. Liu, and X. Wu, "State of charge estimation of lithium-ion batteries using a discrete-time nonlinear observer," *IEEE Transactions on Industrial Electronics*, vol. 64, no. 11, pp. 8557–8565, 2017.

[17] W. M. Haddad and J. Lee, "Finite-time stability of discrete autonomous systems," *Automatica*, vol. 122, p. 109282, 2020.

[18] P. Prasun, S. Kamal, S. Pandey, A. Bartoszewicz, and S. Ghosh, "A minimum operator based discrete-time sliding mode control," *IEEE Transactions on Automatic Control*, 2024.

[19] P. Prasun, S. Pandey, S. Kamal, S. Ghosh, and D. Singh, "Discrete-time gradient systems governed by difference equation with minima," in *2023 31st Mediterranean Conference on Control and Automation (MED)*. IEEE, 2023, pp. 783–788.

[20] P. Prasun, S. Pandey, S. Kamal, S. Ghosh, and X. Xiong, "A minimum operator based discrete-time super-twisting-like algorithm," *IEEE Transactions on Circuits and Systems II: Express Briefs*, 2023.

[21] S. Pandey, S. Kamal, P. Osinenko, S. Parsegov, and D. Singh, "Finite and fixed-time stabilization of discrete-time systems using passivity-based control," *International Journal of Robust and Nonlinear Control*.

[22] V.-H. Duong, H. A. Bastawrous, K. Lim, K. W. See, P. Zhang, and S. X. Dou, "Online state of charge and model parameters estimation of the lifepo4 battery in electric vehicles using multiple adaptive forgetting factors recursive least-squares," *Journal of Power Sources*, vol. 296, pp. 215–224, 2015.